

LINBO QIN, JUN HAN<sup>1</sup>, WANGSHENG CHEN<sup>1</sup>, ZHANZHUANG LIU<sup>1</sup>,  
MENGXIA HE<sup>1</sup>, FUTANG XING<sup>1</sup>

## ENHANCING SO<sub>2</sub> REMOVAL EFFICIENCY BY LIME MODIFIED WITH SEWAGE SLUDGE IN A NOVEL INTEGRATED DESULFURIZATION PROCESS

In China, the sintering process annually emitted around 1.5 million t SO<sub>2</sub>, representing 70% of SO<sub>2</sub> produced from the iron and steel industry. Lime based sorbent was modified with municipal sewage sludge (MSS) and the influence of the modification on the desulfurization efficiency was investigated in a laboratory-scale novel integrated desulfurization (NID) reactor. The properties of modified sorbent were characterized by the Brunauer–Emmett–Teller (BET) analyzer and X-ray fluorescence (XRD) analyzer. BET surface area was increased from 17.48 to 46.68 m<sup>2</sup>·g<sup>-1</sup> when the MSS/lime ratio increased from 0 to 0.08. Ca<sub>4</sub>Al<sub>8</sub>Si<sub>8</sub>O<sub>32</sub>, Ca<sub>1.5</sub>SiO<sub>3.5</sub>, Na<sub>2</sub>Si<sub>2</sub>O<sub>5</sub> and CaSiO<sub>3</sub> found in the modified lime benefited for the increase of the BET surface area and pore volume. The effects of sewage sludge/CaO weight ratio, calcination temperature and hydration time on the desulfurization efficiency were also studied. SO<sub>2</sub> removal efficiency was increased from 88.7% to 97.3% after using the lime modified with sewage sludge.

### 1. INTRODUCTION

SO<sub>2</sub> and NO<sub>x</sub> from many industries such as the coal-burning power plants, iron and steel plants, waste incinerators, etc. [1] are the main causes of acid rain, photochemical smog, and respiratory organ disease. According to the survey report of SO<sub>2</sub> emission in China, the sintering process annually emitted about 1.5 million t of SO<sub>2</sub>, which constituted 70% of SO<sub>2</sub> produced from iron and steel industry [2]. At present, SO<sub>2</sub> emission concentration in the sintering flue gas is 1000–3000 mg/Nm<sup>3</sup> before the flue gas desulfurization devices. With the implementation of new acts or regulations in China, SO<sub>2</sub> removal from the sintering process becomes urgent. For example, *Discharge standard of air pollutants for iron and steel industry* requires that SO<sub>2</sub> emission concentration in

---

<sup>1</sup>College of Resources and Environment Engineering, Wuhan University of Science and Technology, Wuhan 430081, Hubei, P.R. China, e-mail addresses: J. Han hanjun@wust.edu.cn, F. Xing xing\_futang@163.com

the sintering flue gas must be below  $200 \text{ mg}\cdot\text{Nm}^{-3}$  [3]. Therefore, the desulfurization from the sintering flue gas has received widely attention in China.

At present, desulfurization technologies in the sintering plants include the wet desulfurization, semi-dry desulfurization and dry desulfurization [4]. Wet desulfurization technologies have been widely applied due to their high  $\text{SO}_2$  removal efficiency [5]. However, they have such shortcomings as complicated configuration, high operation cost and secondary pollutants [6]. The dry desulfurization technology is attractive because it does not produce secondary pollutants. Nonetheless, low  $\text{SO}_2$  removal efficiency limits its application [7–9]. Semi-dry desulfurization technologies have been developed to avoid the disadvantages of the wet desulfurization and dry desulfurization technology [10]. Novel integrated desulfurization (NID) technology is regarded as one of the promising semi-dry flue gas desulfurization technologies because of its low water consumption, high operation flexibility and low initial investment and operation cost [11]. However, the desulfurization efficiency and Ca-based sorbents utilization efficiency in NID systems were still not high [12–14]. Previous studies reported that Na and K oxides in the sorbents would form NaOH and KOH in NID, which could effectively improve the desulfurization efficiency and the performance of the Ca-based sorbents [15]. Fe and Mn oxides were also expected to have the catalytic ability of the sulfation reaction between Ca and  $\text{SO}_2$  [16]. In the presence of water, active Si and Al in the sorbents would react with hydrated lime and form complex compounds of calcium silicate/aluminate hydrate [17, 18], which caused the increase of the Brunauer–Emmett–Teller (BET) surface area of the sorbents [19, 20].

Sewage sludge is a solid waste, which has high concentration of Na, K, Si, Al, Ca, Fe and Mn [21–24]. Especially, the annual production of sewage sludge in China is about 40 million t, and the disposal of untreated sewage sludge is prohibited. Therefore, lime modified with sewage sludge would benefit for the desulfurization performance and sewage sludge treatment.

In this paper, the desulfurization efficiency by the lime modified with sewage sludge was investigated in a laboratory scale NID system. Meanwhile, the effects of sewage sludge/CaO ratio, calcination temperature and hydration time on the properties of the sorbents and desulfurization efficiency were also studied.

## 2. EXPERIMENTAL

*Materials.* Lime was obtained from Wuhan iron and steel Corp., China. MSS came from a wastewater treatment plant in Wuhan City, China. Before the experiment, the sorbent and MSS were dried, milled and sieved to less than  $74 \mu\text{m}$ . The proximate analysis was characterized by the Elementar (Vario EL III, elementar Analysensysteme GmbH, German). The ultimate analysis of MSS was analyzed according to GB/T 212-2008. The ash components of the sorbent and MSS were analyzed by X-ray fluorescence

(Mode EAGLE III, EDAX Co, America). The chemical and physical characteristics of sorbent and MSS are summarized in Table 1.

Table 1

Chemical and physical characteristics of sorbent and MSS

	Dry ash free [wt. %]				Air dried [wt. %]				
Sewage sludge	42.06	7.45	41.62	7.42	1.45	45.53	2.25	45.39	6.83
Dry ash basis [wt. %]									
	Na <sub>2</sub> O	K <sub>2</sub> O	CaO	SiO <sub>2</sub>	Fe <sub>2</sub> O <sub>3</sub>	Al <sub>2</sub> O <sub>3</sub>	MgO	P <sub>2</sub> O <sub>5</sub>	SO <sub>3</sub>
Sewage sludge	5.31	3.59	15.60	50.80	9.71	7.79	4.74	1.30	1.16
Lime	0.78	0.37	87.01	3.59	2.63	1.74	1.97	1.14	0.37

*Sorbent preparation.* MSS was firstly mixed with lime in the range of weight ratio 0–0.10, and then the mixture was calcined in a muffle furnace at 500–800 °C for 60 min. After the calcination, water was added into MSS/lime mixture to form slurry in the hydration system (water/sorbent weight ratio was 1.8). In the hydration process, the slurry was stirred with a shaker at 150 rpm for 0.5–5.0 h. Meanwhile, the slurry was subsequently heated to 45 °C in a water bath. After the hydration, the slurry was dried in a vacuum oven at 105 °C. Lastly, the dried sorbent was crushed and sieved to less than 74 µm.

Table 2

The preparation conditions of sorbents

Sample	Sewage sludge/CaO ratio	Calcination temperature [°C]	Hydration duration [h]		
S0	0.08	no calcination			
S1	0.00	600			
S2	0.02				
S3	0.04				
S4	0.06				
S5	0.08				
S6	0.10				
S7	0.08	500			
S8		600			
S9		700			
S10		800		2	
S11		600			0.5
S12					1.0
S13					1.5
S14					2.0
S15					3.0
S16			5.0		

The modified sorbents were designated as S0 to S16 according to the preparation condition, as listed in Table 2. S0 represented the modified sorbents without calcination when MSS/lime ratio was 0.08 and the hydration period was 2 h; S1–S6 meant the modified sorbents with MSS/lime ratio in the range of 0–0.10 at 600 °C and 2.0 h hydration time; S7–S10 represented the modified sorbents with the calcination temperature in the range of 500–800 °C when the MSS/lime ratio was 0.08 and the hydration period was 2 h; S11–S16 were the modified sorbents with 0.5–5 h hydration time, 600 °C calcination temperature and 0.08 MSS/lime ratio.

*Characterization.* The BET surface area and pore volume distribution of the lime, sewage sludge and the modified sorbents were measured by the nitrogen physisorption at 77 K with a micromeritics surface area and porosity analyzer (ASAP 2020, American). Prior to the measurements, the samples were heated to 250 °C for degassing. X-ray diffraction patterns (XRD, PANalytical Corp, Holland) were used to characterize the morphologies of the modified sorbents.

*Experimental apparatus.* The diagram of experimental apparatus is shown in Fig. 1. The experimental apparatus consisted of the simulated flue gas system, gas pre-heater,

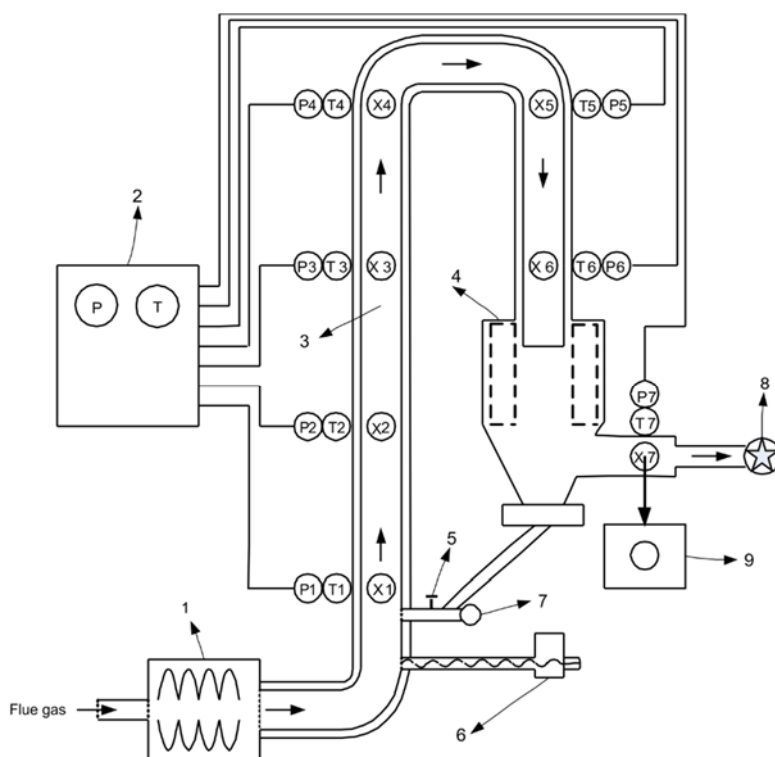


Fig. 1. Diagram of experimental apparatus

De-SO<sub>2</sub> reactor, bag filter and gas analysis system. In the experiments, air from a compressor was mixed with SO<sub>2</sub> from a gas cylinder, and formed the simulated flue gas, and the flow rates of air and SO<sub>2</sub> were controlled with the flow meters. Then the simulated flue gas was heated to pre-determined temperature. The De-SO<sub>2</sub> reactor was made of stainless steel with an internal diameter of 0.05 m and a vertical length of 3.5 m. The sorbent was continuously fed into the De-SO<sub>2</sub> reactor by a screw conveyor with a variable speed. Water was provided by a pump. In the reactor, the sorbent and water formed slurry and reacted with SO<sub>2</sub> in flue gas. Finally, the reacted sorbent carried by flue gas was collected with a bag filter. The residence time of the simulated flue gas in the reactor was about 2 s.

In this study, type-K thermocouples, a Wika pressure transmitter and a Horiba portable gas analyzer (PG 250, Horiba Corp., Japan) were used to record the temperature, pressure and the gas components. The measured locations were labeled points 1–7, as shown in Fig. 1. Points 1–4 were 0, 50, 100 and 150 cm above the inlet of water, respectively. Points 6 and point 5 were 0 and 50 cm above the bag filter, and point 7 was located at the outlet of the bag filter. Temperature and pressure signals were recorded with a Pico technology 8-channel data logger (Model TC-08) and its software. The repeatability and the linear of the portable gas analyzer were less than  $\pm 1\%$  full scan and  $\pm 2\%$  full scan, respectively. In this study, each run was performed 30 min and the average data were used. The experimental conditions are summarized in Table 3.

Table 3

## Experimental conditions

Parameter	Value
Inlet SO <sub>2</sub> concentration, C <sub>in</sub> , mg·Nm <sup>-3</sup>	1400, 2800
Stoichiometric ratio Ca/S	1.4
Stoichiometric ratio H <sub>2</sub> O/CaO	1.8
Inlet gas temperature, T <sub>1</sub> , °C	110
Circulation ratio, Q	60
Flow rate of the simulation flue gas, V, m <sup>3</sup> ·h <sup>-1</sup>	25
Residence time of the simulation flue gas, t, s	2.0

## 3. RESULTS AND DISCUSSION

## 3.1. CHARACTERIZATION OF THE MODIFIED SORBENTS

X-ray diffraction patterns of lime and the modified sorbents are shown in Fig. 2. XRD patterns exhibited strong diffraction peaks at 44.7° and 48.4°, which indicated that there was Ca(OH)<sub>2</sub> in the sorbent. Low intensity peaks of SiO<sub>2</sub> and Fe<sub>2</sub>O<sub>3</sub> were also found. After the calcination, the diffraction peak of Ca(OH)<sub>2</sub> was stronger. At the same

time, the peak intensity of  $\text{Ca}(\text{OH})_2$  was increased with the calcination temperature. In comparison to uncalcined sorbent,  $\text{Ca}_4\text{Al}_8\text{Si}_8\text{O}_{32}$ ,  $\text{Ca}_{1.5}\text{SiO}_{3.5}$ ,  $\text{Na}_2\text{Si}_2\text{O}_5$  and  $\text{CaSiO}_3$  were formed and  $\text{NaOH}$  disappeared when the MSS/lime mixtures were calcined at 600–800 °C. Ogenga et al. [15] stated that the complex compounds in the sorbent were responsible for the increase of BET surface area. High concentration of ferric oxides coupled with  $\text{CaO}$  and silica were benefit for the formation of active desulfurization sorbent.

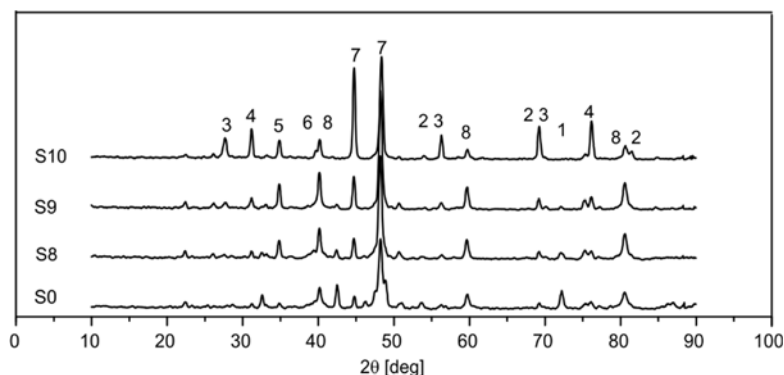


Fig. 2. X-ray diffraction pattern of the modified sorbents:  
 1 –  $\text{NaOH}$ , 2 –  $\text{SiO}_2$ , 3 –  $\text{Ca}_4\text{Al}_8\text{Si}_8\text{O}_{32}$ , 4 –  $\text{Ca}_{1.5}\text{SiO}_{3.5}$ ,  
 5 –  $\text{Na}_2\text{Si}_2\text{O}_5$ , 6 –  $\text{CaSiO}_3$ , 7 –  $\text{Ca}(\text{OH})_2$ ,  $\text{Fe}_2\text{O}_3$

In Table 4 (rows S1–S6) the effect of the MSS/lime ratio on the BET surface area and pore volume of the modified sorbents is visible. All modified sorbents had the higher BET surface area than that of lime. The BET surface area first increased from 17.48 to 46.68  $\text{m}^2\cdot\text{g}^{-1}$  when the MSS/lime ratio increased from 0 to 0.08, and then decreased to 37.89  $\text{m}^2\cdot\text{g}^{-1}$  at 0.10 MSS/lime ratio. The ultramicropore volume and supermicropore volume of the modified sorbents also first increased and then decreased with the increase of MSS/lime ratio. Similarly, the mesopore volume also increased with the increase of MSS/lime ratio, while the macropore volume was independent of the MSS/lime ratio. In Table 4 (rows S7–S10), the effect of the calcination temperature on BET surface area and pore volume of the modified sorbents is demonstrated. All of the modified sorbents calcined at 500–800 °C had the higher BET surface area than that of the MSS/lime without calcination (S0 in Table 4), The BET surface area increased from 39.16 to 53.22  $\text{m}^2\cdot\text{g}^{-1}$  when the calcination temperature increased from 500 to 700 °C, and then decreased to 42.11  $\text{m}^2\cdot\text{g}^{-1}$  under calcination at 800 °C. The ultramicropore volume and supermicropore volume of the sorbents also first increased and then decreased with the increase of the calcination temperature, and the maximum ultramicropore volume and supermicropore volume occurred at 700 °C. On the contrary, the mesopore volume and the macropore volume first decreased and then increased when the calcination temperature increased from 500 to 800 °C. In Table 4 (rows S11–S16), the effect of hydration time on BET surface area and pore volume of the modified sorbents is also visible.

The BET surface area, ultramicropore volume and supermicropore volume of the modified sorbents increased with the increase of the hydration time, whereas the mesopore volume and the macropore volume decreased when the hydration time was in the range of 0.5–5.0 h. In general, upon increasing hydration time, the BET surface area and the pore volume of the sorbents increased.

Table 4

BET surface area and pore volume distribution of the sorbents

Sample	BET surface area [m <sup>2</sup> ·g <sup>-1</sup> ]	Pore volume [cm <sup>3</sup> ·g <sup>-1</sup> ]			
		Ultramicropore (<0.7 nm)	Supermicropore (0.7–2.0 nm)	Mesopore (2.0–50 nm)	Macropore (>50 nm)
Lime	13.66	0.0579	0.0688	0.0097	0.0018
Sewage sludge	9.87	0.0449	0.0556	0.0118	0.0016
S0	18.33	0.0812	0.0762	0.0099	0.0023
S1	17.48	0.0668	0.0713	0.0105	0.0019
S2	22.14	0.0749	0.0766	0.0118	0.0016
S3	37.05	0.1124	0.0900	0.0125	0.0017
S4	43.33	0.0896	0.1020	0.0134	0.0017
S5	46.68	0.1264	0.1301	0.0132	0.0011
S6	37.89	0.0768	0.0911	0.0156	0.0016
S7	39.16	0.1016	0.0912	0.0091	0.0021
S8	46.68	0.1264	0.1301	0.0083	0.0011
S9	53.22	0.1334	0.1356	0.0071	0.0013
S10	42.11	0.1121	0.1023	0.0086	0.0015
S11	39.88	0.0898	0.1021	0.0118	0.0039
S12	42.18	0.1024	0.1132	0.0124	0.0032
S13	44.06	0.1189	0.1276	0.0102	0.0021
S14	46.68	0.1264	0.1301	0.0083	0.0011
S15	47.21	0.1288	0.1324	0.0066	0.0012
S16	47.34	0.1309	0.1367	0.0067	0.0010

The above results can be explained by the two mechanisms. First there was 45.39% of volatile matters in MSS, which was released during the calcination and resulted in the increase of BET area and pore volume. Another reason was that active Si and Al in MSS would react with hydrated lime and form complex compounds of calcium silicate/aluminate hydrate, which were responsible for increasing BET surface area [15].

### 3.2. DESULFURIZATION CHARACTERISTICS OF THE MODIFIED SORBENTS

The effect of MSS/lime weight ratio on SO<sub>2</sub> removal efficiency is shown in Fig. 3. In this run, the MSS/lime weight ratio was 0–0.10, the calcination temperature was 600 °C, and the hydration time was 2 h. Experimental results demonstrated that the desulfurization efficiency rapidly increased with the MSS/lime weight ratio when the MSS/lime

weight ratio was below 0.08, while its further increase had no influence on the desulfurization efficiency. In comparison to lime, the desulfurization efficiency under 0.08 MSS/lime weight ratio increased by 8.5–11.4%. The desulfurization efficiency with lime and modified lime (0.08 MSS/lime weight ratio) was 88.7% and 97.3%, respectively. The increase of the desulfurization efficiency could be attributed to the increase of the BET surface area and pore volume of sorbents [15].

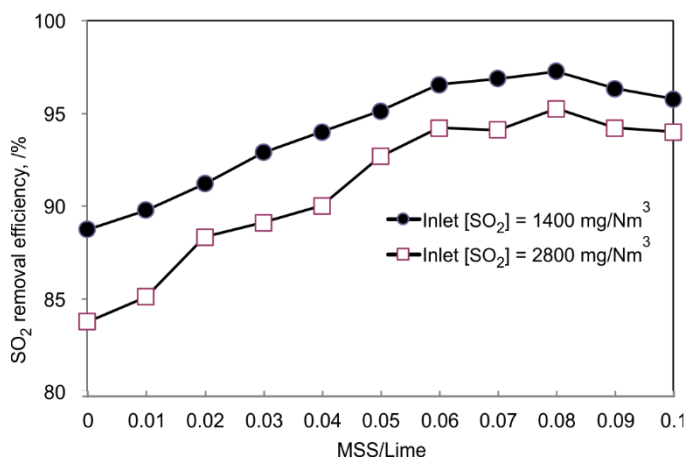


Fig. 3. Effect of MSS/lime weight ratio on the SO<sub>2</sub> removal efficiency

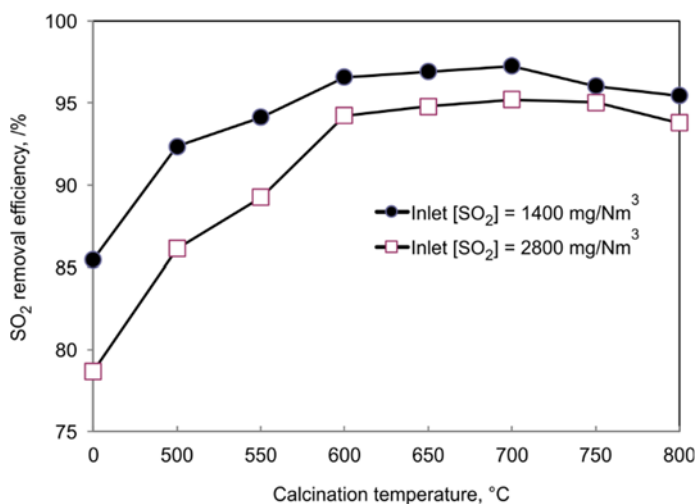


Fig. 4. Effect of calcination temperature on the SO<sub>2</sub> removal efficiency

The effect of the calcination temperature on SO<sub>2</sub> removal efficiency is presented in Fig. 4. The experiments were conducted at the temperature range of 500–800 °C, 0.08 MSS/lime



weight ratio, and 2 h hydration time. SO<sub>2</sub> removal efficiency first increased and then decreased upon increasing temperature, and the maximum desulfurization efficiency occurred at 700 °C. In comparison to MSS/lime calcined at 500 °C, the desulfurization efficiency of MSS/lime calcined at 700 °C was increased by 4.9–9.1%. High calcination temperature promoted thermal decomposition of sewage sludge, which led to the increase of BET surface area and pore volume. However, the sorbent would be sintered and the pores were blocked above 700 °C. Hence, the BET surface area and pore volume was decreased.

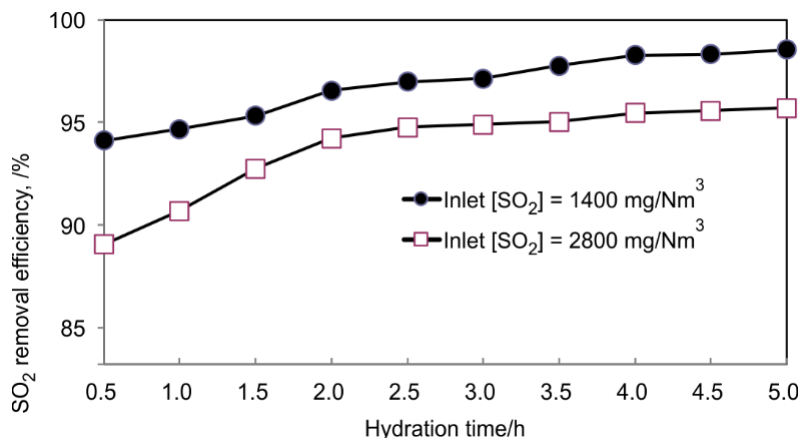


Fig. 5. Effect of hydration time on the SO<sub>2</sub> removal efficiency

Figure 5 demonstrates the effect of hydration time on the SO<sub>2</sub> removal efficiency at 600 °C in the time range of 0.5–5.0 h. The MSS/lime weight ratio was 0.08. The desulfurization efficiency rapidly increased during first 3 hours, and then slightly increased. Fernandez et al. [25] suggested that silica and alumina compounds in the additive could react with Ca(OH)<sub>2</sub> in the slurry, which accounted for the improvement of the reactivity.

### 3.3. SO<sub>2</sub> REMOVAL EFFICIENCY ALONG THE VERTICAL DIRECTION OF THE REACTOR

Figure 6 shows the SO<sub>2</sub> removal efficiency along the vertical direction of the reactor at 600 °C within 2.0 h of hydration time, for 0.08 MSS/lime weight ratio. The monitoring points were located at X1–X7, which corresponded to 0, 0.3, 0.6, 0.9, 1.2, 1.5 and 2.0 s residence time. The desulfurization efficiency at the monitoring points X1–X7 were 3.5, 36.4, 56.3, 82.4, 91.2, 94.1 and 98.7%, respectively. With respect to X6, the desulfurization efficiency at X7 was increased by 4.5%, which meant that the desulfurization efficiency in the bag filter was only 4.5%. It also can be concluded that the desulfurization reaction mainly occurred at 0–1.2 s.

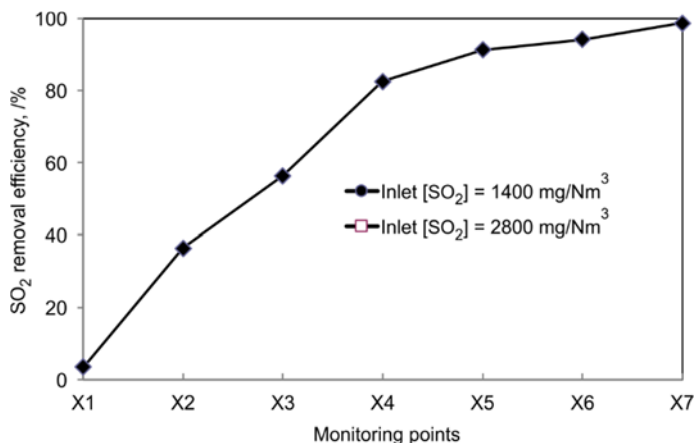


Fig. 6. SO<sub>2</sub> removal efficiency along the vertical direction of the reactor

#### 4. CONCLUSIONS

Lime modified MSS could have high BET surface area and pore volume, which benefits for improving the desulfurization efficiency.

MSS/lime weight ratio, calcination temperature and hydration time had both individual and interactive effects on the BET surface area and pore volume of the sorbents, and the optimum desulfurization parameters were 0.08 MSS/lime weight ratio, 700 °C calcination temperature and 3.0 h hydration time.

In comparison to lime, the desulfurization efficiency with the modified lime could be enhanced by 8.5–11.4% under the optimum parameters.

#### ACKNOWLEDGEMENT

This work was partly supported by the National Natural Science Foundation of China (Grant No. 51476118) and Natural Science Foundation of Hubei Province (2014CFA030&2016AHB025).

#### REFERENCES

- [1] HAN J., KIM H., SAKAGUCHI Y., CHEOL-HO K., YAO H., *The synergetic effect of plasma and catalyst on simultaneous removal of SO<sub>2</sub> and NO<sub>x</sub>*, Asia-Pac. J. Chem. Eng., 2010, 5 (3), 441.
- [2] *China Statistical Yearbook on Environment*, National Bureau of Statistics of China, 2012.
- [3] *Emission standard of air pollutants for sintering and pelletizing of iron and steel industry*, Ministry of Environmental Protection of China, 2012.
- [4] MA X., KANEKO T., XU G., KATO K., *Influence of gas components on removal of SO<sub>2</sub> from flue gas in the semidry FGD process with a powder-particle spouted bed*, Fuel, 2001, 80 (5), 673.
- [5] ZHANG X., WANG N., *Effect of humidification water on semi-dry flue gas desulfurization*, Energy Proc., 2012, 14, 1659.

- [6] WANG N., LUO Z., GAO X., CEN K., *Study of new semi-dry flue gas desulfurization*, J. Power Eng., 2003, 23, 2586 (in Chinese).
- [7] ZHOU Y., PENG J., ZHU X., ZHANG M., *Hydrodynamics of gas–solid flow in the circulating fluidized bed reactor for dry flue gas desulfurization*, Powder Technol., 2011, 205 (1), 208.
- [8] MAROCCO L., MORA A., *CFD modeling of the Dry-sorbent-injection process for flue gas desulfurization using hydrated lime*, Sep. Purif. Technol., 2013, 108, 205.
- [9] WANG X., LI Y., ZHU T., JING P., WANG J., *Simulation of the heterogeneous semi-dry flue gas desulfurization in a pilot CFB riser using the two-fluid model*, Chem. Eng. J., 2015, 264, 479.
- [10] ZHANG Y., WANG T., YANG H., ZHANG H., ZHANG X., *Experimental study on SO<sub>2</sub> recovery using a sodium–zinc sorbent based flue gas desulfurization technology*, Chinese J. Chem. Eng., 2015, 23, 241.
- [11] WANG Y., WANG H., DUAN Y., *Experimental research of NID semi-dry desulfurization of flue gas*, Boiler Technol., 2011, 42 (3), 71.
- [12] LIU H., *Application of NID desulfurization process for WISCO sintering flue gas*, Ind. Safety Environ. Prot., 2011, 7, 13.
- [13] SHIN K., KIM H., KIM Y., LEE H., *Effect of reactivity of quick lime on the properties of hydrated lime sorbent for SO<sub>2</sub> removal*, J. Mater. Sci. Technol., 2009, 25 (3), 329.
- [14] ZHOU Y., ZHU X., PENG J., LIU Y., ZHANG D., ZHANG M., *The effect of hydrogen peroxide solution on SO<sub>2</sub> removal in the semidry flue gas desulfurization process*, J. Hazard. Mater., 2009, 170 (1), 436.
- [15] OGEGA D., MBARAWA M., LEE K., MOHAMED A., DAHLAN I., *Sulfur dioxide removal using South African limestone/siliceous materials*, Fuel, 2010, 89 (9), 2549.
- [16] RENEDO M., FERNANDEZ J., *Kinetic modelling of the hydrothermal reaction of fly ash, Ca(OH)<sub>2</sub> and CaSO<sub>4</sub> in the preparation of desulfurant sorbents*, Fuel, 2004, 83 (4), 525.
- [17] LIU C.-F., SHIH S.-M., LIN R.-B., *Kinetics of the reaction of Ca(OH)<sub>2</sub>/fly ash sorbent with SO<sub>2</sub> at low temperatures*, Chem. Eng. Sci., 2002, 57 (1), 93.
- [18] LIN R.-B., SHIH S.-M., LIU C.-F., *Structural properties and reactivities of Ca(OH)<sub>2</sub>/fly ash sorbents for flue gas desulfurization*, Ind. Eng. Chem. Res., 2003, 42 (7), 1350.
- [19] DAVINI P., *Investigation of the SO<sub>2</sub> adsorption properties of Ca(OH)<sub>2</sub>-fly ash systems*, Fuel, 1996, 75 (6), 713.
- [20] LEE K.T., BHATIA S., MOHAMED A.R., *Preparation and characterization of sorbents modified from ash (waste material) for sulfur dioxide (SO<sub>2</sub>) removal*, J. Mater. Cycles Waste, 2005, 7 (1), 16.
- [21] HAN J., QIN L., YE W., LI Y., LIU L., WANG H., YAO H., *Emission of polycyclic aromatic hydrocarbons from coal and sewage sludge co-combustion in a drop tube furnace*, Waste Manage. Res., 2012, 30 (9), 875–882.
- [22] LIU H., ZHANG Q., HU H., LIU P., HU X., LI A., YAO H., *Catalytic role of conditioner CaO in nitrogen transformation during sewage sludge pyrolysis*, Proc. Combust. Inst., 2015, 35 (3), 2759.
- [23] HU H., LIU H., CHEN J., YAO H., LI A., LOW F., ZHANG L., *Speciation transformation of arsenic during municipal solid waste incineration*, Proc. Combust. Inst., 2015, 35 (3), 2883.
- [24] LIU H., ZHANG Q., XING H., HU H., LI A., YAO H., *Product distribution and sulfur behavior in sewage sludge pyrolysis. Synergistic effect of Fenton peroxidation and CaO conditioning*, Fuel, 2015, 159, 68.
- [25] FERNÁNDEZ J., RENEDO J., GAREA A., VIGURI J., IRABIEN J.A., *Preparation and characterization of fly ash/hydrated lime sorbents for SO<sub>2</sub> removal*, Powder Technol., 1997, 94, 133.